Time Scales of Land Surface Hydrology

AIHUI WANG

Department of Atmospheric Sciences, The University of Arizona, Tucson, Arizona, and Institute of Atmospheric Physics, Chinese Academy of Sciences, Beijing, China

XUBIN ZENG

Department of Atmospheric Sciences, The University of Arizona, Tucson, Arizona

SAMUEL S. P. SHEN

Department of Mathematics and Statistics, University of Alberta, Edmonton, Alberta, Canada

QING-CUN ZENG

Institute of Atmospheric Physics, Chinese Academy of Sciences, Beijing, China

ROBERT E. DICKINSON

School of Earth and Atmospheric Sciences, Georgia Institute of Technology, Atlanta, Georgia

(Manuscript received 1 November 2005, in final form 21 December 2005)

ABSTRACT

This paper intends to investigate the time scales of land surface hydrology and enhance the understanding of the hydrological cycle between the atmosphere, vegetation, and soil. A three-layer model for land surface hydrology is developed to study the temporal variation and vertical structure of water reservoirs in the vegetation–soil system in response to precipitation forcing. The model is an extension of the existing one-layer bucket model. A new time scale is derived, and it better represents the response time scale of soil moisture in the root zone than the previously derived inherent time scale (i.e., the ratio of the field capacity to the potential evaporation). It is found that different water reservoirs of the vegetation–soil system have different time scales. Precipitation forcing is mainly concentrated on short time scales with small low-frequency components, but it can cause long time-scale disturbances in the soil moisture of root zone. This time scale increases with soil depth, but it can be reduced significantly under wetter conditions. Although the time scale of total water content in the vertical column in the three-layer model is similar to that of the one-layer bucket model, the time scale of evapotranspiration is very different. This suggests the need to consider the vertical structure in land surface hydrology reservoirs and in climate study.

1. Introduction

Hydrological cycling between the atmosphere, vegetation, and soil plays an important role in land surface processes. Understanding its variability and relationship to atmospheric processes on various time scales will help better understand the impact of soil moisture on weather and climate and better manage water resources. One of the important aspects of the surface hydrological cycle is how the land surface components (soil moisture, evapotranspiration, and runoff) respond to the precipitation forcing (Vinnikov and Yeserkepova 1991; Vinnikov et al. 1996; Scott et al. 1997; Koster and Suarez 1996, 2001; Wu et al. 2002; Dickinson et al. 2003).

Suppose that precipitation is the only water source of the land surface. The rainfall arriving at the top of vegetation either is intercepted by foliage, or falls through canopy to ground. The intercepted part reduces the

Corresponding author address: Aihui Wang, Dept. of Atmospheric Sciences, 1118 E. 4th St., P.O. Box 210081, The University of Arizona, Tucson, AZ 85721.
E-mail: ahwang@atmo.arizona.edu

supply of water to the soil. In addition, the vegetation foliage reduces soil evaporation by reduction of the net radiation through shadowing of leaves (Scott et al. 1995). On the other hand, water is extracted from the root zone to foliage for transpiration, and the moisture in soil surface layer and root zone also interact via infiltration. If the intensity of precipitation is large enough, some part of the rainfall can directly go into the root zone through macropores. In turn, evapotranspiration is always the main mechanism to feed back water into the atmosphere (Entekhabi et al. 1992), and it may affect the precipitation statistics (Koster and Suarez 1996). In general, some parts of precipitation are stored in the vegetation–soil reservoir, and other parts must be balanced by runoff and evapotranspiration (Milly 1993). These are the major mechanisms of hydrological interactions in the atmosphere–vegetation–soil system.

Because of the complexity of nonlinear and multiple interactive processes included in the hydrological system of atmosphere–vegetation–soil, few theoretical investigations have addressed the above mechanisms in the literature, and most of them considered the one-layer bucket model (Manabe 1969), except for some brief notes on general characters of time scales in multiple layers of soil (Dickinson et al. 2003). Many important questions are still open and need further study. The following questions are crucial: What are the essential differences between a model without vertical structure (one-layer model) and a model with vertical structure (a multiple-layer model)? How do the vertical structures and the mutual interactions between layers influence the temporal structure of the evolutionary process? How can we improve the estimation of soil moisture response time scales? With regard to these questions, studies using global models (Delworth and Manabe 1988, 1989; Koster and Suarez 2001) and observational data (Vinnikov and Yeserkepova 1991; Vinnikov et al. 1996; Entin et al. 2000; Wu et al. 2002) have shown that soil moisture memory is significantly longer than most of the atmospheric processes associated with weather systems. Further, soil moisture memory significantly depends on the characteristics of atmospheric processes such as the statistics of precipitation. In particular, Delworth and Manabe (1988) demonstrated that short-time-scale precipitation fluctuations could be filtered to provide long-time-scale anomalies of soil moisture. They also indicated that the time scale of soil moisture anomalies in the absence of precipitation forcing is proportional to the ratio of field capacity of soil layer to the potential evaporation, and this time scale is identical to the decay time scale of soil moisture when evaporation is a linear function of soil moisture. This theoretical conclusion was confirmed by using an empirical dataset in the Soviet Union (Vinnikov and Yeserkepova 1991).

In this paper, we introduce a three-layer model as an extension of the simple bucket model. It is simple enough to allow rigorous mathematical analysis and realistic enough to explain the important results from previous global modeling studies and the analysis of observational data. Section 2 analyzes the time-scale variations of precipitation and soil moisture in the one-layer model and improves the original theory of Delworth and Manabe (1988). Section 3 extends the one-layer model to a three-layer model. Section 4 develops theoretical methods suitable for multilayer models and describes their application to the analyses of temporal-vertical structures in the three-layer model. Section 5 provides the design of numerical simulations. Simulation results and their comparisons with theoretical analyses and previous studies in sections 2 and 4 are shown in section 6. Conclusions are given in section 7.

2. Time-scale analysis of one-layer model

To investigate the temporal variations of land surface hydrology, we first examine the simplest model, the one-layer bucket water balance model (Manabe 1969). For a column of soil and vegetation, its water balance equation can be written as

$$\frac{dW}{dt} = P - E - R, \tag{1}$$

where W is the total water stored within the column, P is the precipitation, E is the evapotranspiration, and R is the surface runoff and drainage. The evapotranspiration term E is always one of the leading terms and is assumed to be a function of W; R only occurs when water in the vegetation–soil reservoir is supersaturated. Therefore, (1) indicates that the vegetation–soil water reservoir is an open (due to P) and diffusive (due to E and R) system, which typically includes multiple time scales. Here we would extend previous studies to give a more systematic analysis of these time scales.

To quantify the temporal variations of land surface components, we introduce characteristic scales W^*, E^*, and P^* for W, E, and P, respectively. Then, $T^* = W^*/E^*$ represents the characteristic time scale in the temporal variation of water stored in vegetation and soil for the given atmosphere–land condition in the absence of rainfall. Delworth and Manabe (1988) took W^* and E^* as the field capacity and the potential evaporation (or the potential evapotranspiration when the soil surface is covered by vegetation) respectively, and further assumed that evaporation is proportional to W/W^* if the

soil is not too wet. They also demonstrated that T^* corresponds to the e-folding time for the damping of W in the linear system. The response time scale determined by this method is only a first-order approximation and should be further improved in the nonlinear system. In the following, T^* denotes an inherent time scale since it does not depend on atmospheric forcing, and the e-folding denotes time as response time scale.

Under precipitation forcing, there is another time scale related to W variations in response to the external input, that is, precipitation $P(t)$. Consider a highly idealized precipitation time series

$$P(t) = P_\omega e^{i\omega t}, \tag{2}$$

where P_ω is the amplitude and ω is the frequency. It is assumed that E is a monotonic function of W. Substituting (2) into (1), it can be shown that in the case of $2\pi/\omega < T^*$, the temporal variation of W cannot effectively adjust to such high-frequency input, and it maintains its inherent variation with time scale T^* superimposed upon small fluctuations with time scale $2\pi/\omega$. However, in the case of $2\pi/\omega \geq T^*$, after the initial signal is sufficiently decayed, both W and $E + R$ are mainly represented as forced oscillations with low frequency.

In general, $P(t)$ can be described by its spectral distribution

$$P(t) = \int_{-\infty}^{+\infty} P_\omega e^{i\omega t}\, d\omega. \tag{3}$$

The above analyses indicate that when the spectra of $P(t)$ are in the high-frequency domain, that is, $\omega > 2\pi/T^*$, E (or $E + R$) also has almost the same spectral distribution as P_ω, and the high-frequency components in W are negligible. For the low-frequency components of $P(t)$, that is, $\omega \leq 2\pi/T^*$, W, E, and R all respond to P in their evolutionary processes.

From the above analyses, (1) can be taken as a "low pass" filter. The response of W to low-frequency inputs is more effective, and W always possesses low-frequency components even though the spectra of P are concentrated in the high-frequency domain. Therefore, the high-frequency input P leads to a statistical equilibrium state with small amplitude but fast fluctuations of E (or $E + R$) and relatively large amplitude but low-frequency harmonics of W. This is the major mechanism for the reddening of the response spectra relative to the high-frequency input.

If $E + R$ is a linear function of W, the above analyses can be summarized by an analytical and compact mathematical formula. This has been provided in Delworth and Manabe (1988) and Dickinson et al. (2003) based on the concept and method developed by Hasselman (1976) in the design of statistical climate model. However, no compact analytical formula has been reported in the past for the general nonlinear case unless E is locally linearized.

Here we extend the above analysis to the general nonlinear case by using the local linearization method. It is convenient to divide variables into the perturbations (W', E', R', and P') and the long time means ($\overline{W}$, $\overline{E}$, $\overline{R}$, and $\overline{P}$), and rewrite (1) as

$$\frac{dW'}{dt} = P' - E' - R'. \tag{4}$$

With slight modification of the formula of Serafini and Sud (1987), the evaporation E from the available soil moisture W within a single column of vegetation and soil can be given as

$$E = E^*(1 - e^{-\sigma W/W^*})(1 - e^{-\sigma})^{-1} \equiv E^* h(y), \tag{5}$$

where $y \equiv W/W^*$, W^* is the maximum available soil moisture (the soil moisture difference between the field capacity and wilting point of the soil), E^* is the potential evapotranspiration, and the free parameter σ is usually 1–3 depending on vegetation types. The function $h(y)$ can be linearized as $h(y) \approx h(\bar{y}) + h_0(\bar{y})y'$ with $y' \equiv W'/W^*$ and $h_0(\bar{y}) = dh(\bar{y})/dy$, and the mean value, $\overline{E}$, can be written as

$$\overline{E} = E^* h(\bar{y}), \tag{6}$$

where $\bar{y} \equiv \overline{W}/W^*$.

Considering $E = \overline{E} + E'$, we have

$$E' = E^* \alpha \bar{y} \frac{W'}{\overline{W}} \equiv E^{**} \frac{W'}{W}, \tag{7}$$

where $\alpha = \sigma e^{-\sigma\bar{y}}/(1 - e^{-\sigma})$. Denoting $\overline{W}$ as W^{**} and the corresponding actual response time scale as T^{**} for the convenience in the comparison, we have

$$T^{**} = \frac{W^{**}}{E^{**}} = \alpha^{-1} T^*. \tag{8}$$

While T^* is a constant, T^{**} varies with $\bar{y}$ and $T^{**} \approx T^*$ only when $\bar{y}$ is intermediate. Let W' and P' be represented in the spectral form with amplitudes A_ω and A_p respectively along with the frequency ω and neglecting R', then (4) yields

$$|A_w|^2 = |A_p| \frac{|T^{**}|^2}{1 + (\omega T^{**})^2}. \tag{9}$$

This is the same equation as obtained by Delworth and Manabe (1988) and Dickinson et al. (2003) except with T^{**} replacing T^*. Since α and T^{**} depend on $\bar{y}$, the

separating frequency $\omega = (T^{**})^{-1}$ is a slowly varying quantity in the nonlinear case.

3. A three-layer model

Water stored in different layers of the vegetation–soil system has different temporal variations for the precipitation forcing, and the one-layer model in (1) cannot quantitatively distinguish the response time scales. To adequately represent this complexity, a model should include at least three layers: the vegetation canopy, c, the surface soil layer, s, and the root zone of the soil, r (hereafter the subscript $i = c$, s, and r denote canopy, surface soil layer, and root zone, respectively). Here we develop a modified three-layer water balance model as a direct extension of (1) and (4) rather than as a simplification of current comprehensive and complicated land surface models (e.g., Zeng et al. 2002). Water in the top two layers directly interacts with the atmosphere. The bottom layer includes most of vegetation roots, and its water content is thus the main source for plant transpiration. Based on water mass conservation, the governing equations are

$$\frac{dW_c}{dt} = P_c + E_r - E_c - R_c, \tag{10}$$

$$\frac{dW_s}{dt} = P_s + R_c - E_s - R_s - Q_{sr}, \quad \text{and} \tag{11}$$

$$\frac{dW_r}{dt} = P_r + \nu R_s - E_r - R_r + Q_{sr}, \tag{12}$$

where W_i, P_i, and E_i, respectively, denote the water content, precipitation partition, and evapotranspiration (evaporation and transpiration) in different layers; R_c is the outflow from canopy; R_s includes two parts: surface runoff $(1 - \nu)R_s$ and infiltration from s layer to r layer νR_s. Here ν $(0 \le \nu \le 1)$ is a fraction depending on soil texture; R_r is the root zone drainage; and Q_{sr} represents the conductive (diffusive) transfer of water between the s layer and r layer.

Precipitation P is partitioned into three parts P_i $(I = c, s, r)$, in which $P_c = \min(P_c^*, P)$ is the part intercepted by canopy, $P_s = \min(P_s^*, P - P_c)$ is the part held by surface soil layer, and $P_r = P - P_c - P_s$ is the part that directly penetrates into root zone of soil in the case of heavy rain due to the macropores in the soil. Here, P_c^* and P_s^* are the maximum precipitation that c layer and s layer can hold. They depend on the vegetation characteristics and soil properties. Note that the P_r term is also a kind of infiltration but different from νR_s since they are from different sources and have different spectral distributions. The introduction of the P_r term implies that the direct influence of atmosphere to deep soil is taken into account in the model. Further discussion of P_r will be given in section 6.

Applying (5) to the three layers yields

$$E_i = E_i^*(1 - e^{-\sigma_i W_i/W_i^*})(1 - e^{-\sigma_i})^{-1} \equiv E_i^* h_i(y_i), \quad (i = c, s, r), \tag{13}$$

where E_i^* is the potential evapotranspiration, W_i^* is upper bound of water content (field capacity) of ith layer, $y_i \equiv W_i/W_i^*$, and σ_i could be different in different layers. In (10) and (13), E_c includes evaporation from wet leaves and transpiration from dry foliage, E_s is the evaporation from surface layer of soil, and E_r is the soil water extracted by roots and transferred to the canopy. Basically, E_r directly becomes transpiration in most cases, but some part of E_r can be also stored in the leaf in some cases.

The interaction term Q_{sr} between two soil layers can be parameterized as

$$Q_{sr} = \lambda^{-1}\overline{D}_{sr}\left(\frac{W_s}{D_s^*} - \frac{W_r}{D_r^*}\right), \tag{14}$$

where D_s^* and D_r^* are the thickness of s layer and r layer, respectively, $\overline{D}_{sr} \equiv D_s^* D_r^*/(D_s^* + D_r^*)$, and λ is the damping time scale. In the absence of the sources and sinks (i.e., P, E, and R are all absent), $W_s/D_s^* - W_r/D_r^*$ decays to e^{-1} of its initial value during λ time due to the conductive transfer Q_{sr}. It is also assumed that $W_s^*/D_s^* = W_r^*/D_r^*$, which implies that there is no conductive interaction when volumetric soil water contents in both layers are the same.

To compare the three-layer model with the one-layer model, we combine (10)–(12) to obtain

$$\frac{dW}{dt} = P - E - R, \tag{15}$$

where $W \equiv W_c + W_s + W_r$, $E \equiv E_c + E_s$, and $R \equiv (1 - \nu)R_s + R_r$. Equation (15) is equivalent to the one layer-model governed by (1).

4. Time-scale analysis of the three-layer model

In this three-layer model there are several characteristic time scales: an external forcing (P) time scale T_f^*, an internal time scale T_q^* determined by the conductive transport Q_{sr}, and three inherent time scales T_i^* $(i = c, s, \text{and } r)$, which is similar to T^* in section 2. Furthermore, we can even define three other time scales T_{fi}^* due to the partitioning of P into P_i $(i = c, s, \text{and } r)$. It is obvious that T_{fc}^* is the same as T_f^*, and T_{fs}^* and T_{fr}^* depend on the spectral distribution of P_s and P_r, respectively. These multiple time scales imply that the tem-

poral variation of the three-layer model is more complicated (than the one-layer model) and can be irregular.

Similar to the one-layer model, the first-order approximation of the inherent time scales T_i^* for ith layer can be taken as

$$T_i^* = W_i^*/E_i^* \quad (i = c, s, r). \tag{16}$$

For the same atmospheric conditions, E_i^* is of the same order of magnitude, but this does not mean $E_c \approx E_s \approx E_r$. On the other hand, W_c^* is two orders of magnitude smaller than W_s^* and W_r^*, and $W_s^* < W_r^*$ due to $D_s^* < D_r^*$. Hence $T_c^* \ll T_s^* < T_r^*$.

On the other hand, the inherent time scale T^* for (15) is as follows:

$$\begin{aligned} T^* &= (W_c^* + W_s^* + W_r^*)/(E_c^* + E_s^*) \\ &\approx (W_s^* + W_r^*)/(E_c^* + E_s^*). \end{aligned} \tag{17}$$

From (16) and (17), we can derive the following relationship:

$$T_s^* < T^* < T_r^*, \tag{18}$$

which means the one-layer model would shift some part of low-frequency variations from root zone into surface layer. Roughly, the time scale $T_q^* = \lambda$ from (14) is about 10–15 days, T_s^* 10–30 days, and T_r^* 2–6 months.

Equations (11) and (12) indicate that the temporal variation of W_s and W_r is affected by E_s and E_r as well as other processes. Therefore the response time scale of W_s and W_r can be different from T_s^* and T_r^*, respectively.

Also note that 1) the existence of the c layer does not directly affect the hydrological dynamics in the s layer and the r layer except reducing the precipitation available to the soil from P to $P - P_c + R_c$ and $(P_c - R_c)/P$ is very small; 2) the r layer directly affects the c layer by the water supply through E_r; and 3) the s layer and r layer are mutually interactive through conductive transfer and infiltration of water. Therefore we can modify the inherent time scales for s layer and r layer by the use of only (11) and (12) with a described $P_s + R_c$.

In the following analytical investigation of time scales, for generality, runoff R_s and R_r are parameterized as

$$R_i = R_i^* g_i(y_i) \quad (i = s, r), \tag{19}$$

where R_i^* is the maximum value (upper bound) of R_i, $y_i \equiv W_i/W_i^*$ and g_i $(0 \le g_i \le 1)$ is a continuous and monotonical function of y_i so that runoff is still allowed within unsaturated soil. Equations (11) and (12) then are locally linearized with respect to long time means $(\overline{W}_i, \overline{P}_i)$, $i = s, r$. Thus we have the following nondimensional equations:

$$\frac{dy_s'}{d\tau} = \overline{M}_{\mathrm{oi}} m_s \pi_s' - \alpha_s y_s' + \beta_s y_r', \tag{20}$$

$$\frac{dy_r'}{d\tau} = \overline{M}_{\mathrm{oi}} m_r \pi_r' + \beta_r y_s' - \alpha_r y_r', \tag{21}$$

where

$$y_s' \equiv W_s'/W_s^*,\ y_r' \equiv\equiv W_r'/W_r^*,\ \pi_s' \equiv P_s'/P,\ \pi_r' \equiv P_r'/P, \tag{22}$$

$$\tau \equiv t/T_{rs}^*, \quad \text{and} \quad T_{rs}^* \equiv (T_s^* T_r^*)/(T_s^* + T_r^*). \tag{23}$$

All the coefficients in the right-hand side are dimensionless, $\overline{M}_{\mathrm{oi}}$ is the moisture index,

$$\overline{M}_{\mathrm{oi}} \equiv \overline{P}/E_s^*, \tag{24}$$

and

$$m_s = (\tau_s^*)^{-1},\ m_r = \varphi_{rs}/\tau_r^*, \tag{25}$$

$$\alpha_s = (\alpha_{s1} + r_s^* \gamma_s + \tau_{\lambda s}^* d_s^{-1})/\tau_s^*,\ \beta_s = (\tau_{\lambda s}^* w_{sr} d_r^{-1})/\tau_s^*, \tag{26}$$

$$\alpha_r = (\alpha_{r1} + r_r^* \gamma_r + \tau_{\lambda r}^* d_r^{-1})/\tau_r^*,$$

$$\beta_r = (\nu \varphi_{rs} r_s^* \gamma_s + \tau_{\lambda r}^* w_{sr}^{-1} d_s^{-1})/\tau_r^*, \tag{27}$$

where

$$\begin{aligned} &\tau_s^* \equiv T_s^*/T_{rs}^*,\ \tau_r^* \equiv T_r^*/T_{rs}^*,\ \tau_{\lambda s}^* \equiv T_s^*/\lambda,\ \tau_{\lambda r}^* \equiv T_r^*/\lambda, \\ &\varphi_{rs} \equiv E_s^*/E_r^*,\ w_{sr} \equiv W_r^*/W_s^*,\ r_s^* \equiv R_s^*/E_s^*,\ r_r^* \equiv R_r^*/E_r^*, \\ &\alpha_{s1} \equiv dh_s(\overline{y}_s)/dy_s,\ \alpha_{r1} \equiv dh_r(\overline{y}_r)/dy_r,\ \gamma_s \equiv dg_s(\overline{y}_s)/dy_s, \\ &\gamma_r \equiv dg_r(\overline{y}_r)/dy_r,\ d_s^{-1} \equiv \overline{D}_{sr}/D_s^*, \quad \text{and} \quad d_r^{-1} \equiv \overline{D}_{sr}/D_r^*. \end{aligned} \tag{28}$$

Each dimensionless parameter has a definite physical meaning. For instance, φ_{rs} is the ratio of potential evaporation of the s layer to that of the r layer.

It is difficult to compute the e-folding time scale from (20) or (21) that contains two variables. Therefore we transform them into two equations, each of which consists of one variable only:

$$\frac{dz_j'}{d\tau} = -\alpha_j z_j' + f_j' \quad (j = 1, 2), \tag{29}$$

where

$$z_j' = \alpha_{js} y_s' + \alpha_{jr} y_r' \quad \text{and} \tag{30}$$

$$f_j' = (\alpha_{js} m_s \pi_s' + \alpha_{jr} m_r \pi_r') \overline{M}_{\mathrm{oi}} \quad (j = 1, 2). \tag{31}$$

In these equations $-\alpha_1$ and $-\alpha_2$ are the two eigenvalues of the matrix

TABLE 1. Parameters used in the three-layer model, as inferred from observational data in the temporal semiarid grassland in northern China (Jiang 1988; Zeng et al. 2004).

$\overline{P}$ (cm day^{-1})	ν	λ (day)	i	P_i^* (cm day^{-1})	W_i^* (cm)	E_i^* (cm day^{-1})	D_i^* (cm)	σ_i
			c	0.1	0.02	0.2	—	1.3
0.33	0.3	15	s	1.0	2	0.2	5	1.3
			r	—	16	0.1	40	1.3

$$\begin{bmatrix} -\alpha_s & \beta_r \\ \beta_s & -\alpha_r \end{bmatrix},$$

and $(\alpha_{1s}, \alpha_{1r})$ and $(\alpha_{2s}, \alpha_{2r})$ are the two corresponding normalized eigenvectors, respectively. In general all α_j, α_{js}, and α_{jr} are real numbers, and $\alpha_j > 0$, $(j = 1, 2)$. From (20), (21), (24), and (25), the coefficients α_j $(j = 1, 2)$ can be solved

$$\alpha_1 = \frac{1}{2}\{(\alpha_s + \alpha_r) + [(\alpha_s - \alpha_r)^2 + 4\beta_s\beta_r]^{1/2}\}, \quad (32)$$

$$\alpha_2 = \frac{1}{2}\{(\alpha_s + \alpha_r) - [(\alpha_s - \alpha_r)^2 + 4\beta_s\beta_r]^{1/2}\}. \quad (33)$$

The e-folding dimensionless time scale for z_i' is α_i^{-1} $(i = 1, 2)$, and the two response time scales in (29) are

$$T_1^{**} \equiv \alpha_1^{-1} T_{rs}^* \quad \text{and} \quad T_2^{**} \equiv \alpha_2^{-1} T_{rs}^*,$$

rather than the first-order approximation T_s^* and T_r^* in (16). Note that the functional form of (34) is similar to (8).

Taking the parameters as listed in Table 1, various time scales and parameters can be computed, as given in Tables 2 and 3 . Because α_{2r} is much larger than α_{2s} in (30), T_2^{**} effectively provides a new estimate of the time scale of the r layer, and based on numerical simulations, it is better than T_r^* from (16) (see section 6). On the other hand, the difference between T_1^{**} and T_s^* is small (see Table 2); both could represent the time scale of the s layer. It needs to be emphasized that while T_s^* and T_r^* in (16) are independent of precipitation input, our new time scale T_2^{**} does depend upon the mean soil water [based on (26)–(28) and (33)] and hence precipitation.

Now we investigate the response of soil moisture anomaly in (29)–(31) to the input of precipitation anomaly in (22). Assume

$$\pi_s' = A_{\pi s} e^{i\omega t}, \ \pi_r' = A_{\pi r} e^{i\omega t}, \quad (35)$$

where $A_{\pi s}$ and $A_{\pi r}$ are real numbers. Then (31) can be rewritten as

TABLE 2. Derived time scales using the parameters listed in Table 1.

Time scales	Values (days)
T_s^*	10
T_r^*	160
T_q^*	15
T_{rs}^*	9
T_1^{**}	8
T_2^{**}	121

$$f_j' = A_{fj} e^{i\omega t}, \ A_{fj} = \overline{M}_{\text{oi}}(\alpha_{js} m_s A_{\pi s} + \alpha_{jr} m_r A_{\pi r}). \quad (36)$$

Equations (29) and (36) yield

$$z_j' = A_{zj} e^{i(\omega\tau - \psi_j)}, \quad (37)$$

where A_{fj} and A_{zj} are taken as real numbers:

$$|A_{zj}|^2 = \alpha_j^{-2} \frac{|A_{fj}|^2}{[1 + (\omega/\alpha_j)^2]} \quad \text{and} \quad (38)$$

$$\psi_j = \arctan\left(\frac{\omega}{\alpha_j}\right). \quad (39)$$

Evidently, (38) is the direct extension of (9). Assuming $\pi_s'/\pi_r' = \overline{P}_s/\overline{P}_r$, and taking ω as the time scale of $2T_1^{**}$, we have $\psi_1 = 0.46$ and $\psi_2 = 1.44$ from (39). Taking ω as the time scale of $1.5T_2^{**}$, we have $\psi_1 = 0.04$ and $\psi_2 = 0.59$. In either case, $T_2^{**} > T_1^{**}$ (Table 2), and hence $\psi_2 > \psi_1$ in agreement with the data analysis of Wu et al. (2002).

5. The design of numerical experiments

For illustration we have carried out some numerical experiments by using the three-layer model. Daily precipitation is the only model-required external input. For simplicity, the probability density function (PDF)

TABLE 3. Dimensionless quantities in the s layer and r layer using the parameters listed in Table 1.

Dimensionless parameters	Values
α_s	1.2
α_r	0.11
β_s	0.56
β_r	0.07
α_1	1.2
α_2	0.076
α_{1s}	0.9
α_{1r}	−0.44
α_{2s}	0.06
α_{2r}	0.98

of daily precipitation intensity in rainy days is represented by an exponential function

$$f(p) = \frac{1}{\tilde{p}} \exp\left(-\frac{p}{\tilde{p}}\right), \tag{40}$$

where p is the daily precipitation, and $\tilde{p}$ is the prescribed mean daily precipitation for the rainy days. It is also assumed that rainfall occurs 50% of the days over a typical midlatitude grassland region, so that the climatological mean $\bar{p} = \tilde{p}/2$. For instance, (40) is found to reasonably fit the observed summer precipitation over Illinois (not shown). Under these assumptions, the random precipitation time series is generated. For other regions (e.g., monsoon regions), both the occurrence of precipitation (OP) in (40) and $\tilde{p}$ need to be adjusted. Furthermore, similar to Delworth and Manabe (1988), seasonal variation of precipitation is not considered here by taking a constant $\bar{p}$.

Mean daily precipitation $\bar{p}$ and other required parameters in the numerical experiments are listed in Table 1. The time step is taken as 0.1 day, but we focus on the analysis of daily averaged evaporations and water contents for each layer. The model sensitivity to initial conditions is also studied by employing "dry" and "wet" initial conditions respectively. The initial water contents of all the three layers are set as slightly larger than zero in the dry condition, and as their saturated values in the wet condition. After the model has run for a long enough time (approximately after 12 months), the time series of water contents in each layer converge in these two simulations. Without loss of generality, in the following simulations the initial condition is set as wet, and the daily model output after the first 12 months is analyzed.

In our numerical simulations, only the runoff from oversaturation is considered. In other words, $g_i = 1$ for $y_i \geq 1$ and $g_i = 0$ for $y_i < 1$ in (19). This is similar to the assumption used in Noilhan and Planton (1989). Sensitivity of our results to the runoff formulation will also be briefly addressed later.

Two statistical methods (i.e., spectral analysis and autocorrelation analysis) are adopted to analyze the temporal variations of the time series. The first one is used to analyze the spectra of precipitation, water content, and evaporation for different layers. The second is used to study the sensitivity of the time scale of soil moisture in root zone to some model parameters.

Delworth and Manabe (1988) used the first-order Markov process to demonstrate soil moisture memory when they modeled soil moisture variability in the Geophysical Fluid Dynamics Laboratory's (GFDL) atmospheric general circulation model (AGCM). Even though the Markovian framework has some limitations (Koster and Suarez 2001), it captures the basic feature of soil moisture as a red-noise process responding to the short-term atmosphere forcing and provides a single parameter as the measure of soil moisture memory (Wu and Dickinson 2004).

By using the least squares method, the autocorrelation function $r(t)$ of the simulated time series of soil moisture can be approximated as (Delworth and Manabe 1988; Vinnikov and Yeserkepova 1991; Vinnikov et al. 1996)

$$r(t) = \exp(-t/T), \tag{41}$$

where t is the time lag, and T is the e-folding time scale. By using linearized equations, the temporal variation of soil moisture can be represented as a first-order Markov process. Then $r(t)$ is exactly governed by (41), and T is indeed the time scale of the soil moisture. While T represents a reasonable measure of soil moisture memory, it is empirically obtained from the soil moisture time series (rather than from land surface parameters). In contrast, inherent time scales [e.g., (16)] and response time scale [e.g., (34)] discussed in this paper are derived based on climate conditions and land parameters at a given region and hence have clear physical meanings. In the next section, T_2^{**} for (34) and T_r^* for (16) will be compared to see which is closer to T_r of the root zone soil water.

6. Analyses of the numerical results

a. Analysis of W_r and precipitation

Figure 1 shows the variations of the response time scales of W_r [as computed from (41)] to the precipitation forcing in 300 independent simulations. These simulations differ only in the random number used to describe $f(p)$ in (40), while keeping the daily mean precipitation constant. The time scale of W_r is sensitive to the random sequence of precipitation (Fig. 1a), but in most of the simulations it is concentrated within the range of 50 to 100 days (Fig. 1b). The median response time scale (denoted as T_r) is 74 days with the 10th and 90th percentiles being 35 and 128 days, respectively. Using the soil observation data over the midlatitude grassland and agricultural areas in Eurasia and American continents, Entin et al. (2000) estimated that the time scales for top 1 m vary from 1 to 2.5 months, compatible with the response time scales in Fig. 1. The median value of 74 days in Fig. 1 is just half the inherent time scale $T_r^* = W_r^*/E_r^* = 160$ days. This is not surprising because T_r^* does not explicitly consider the influence of precipitation on the response time scale of soil

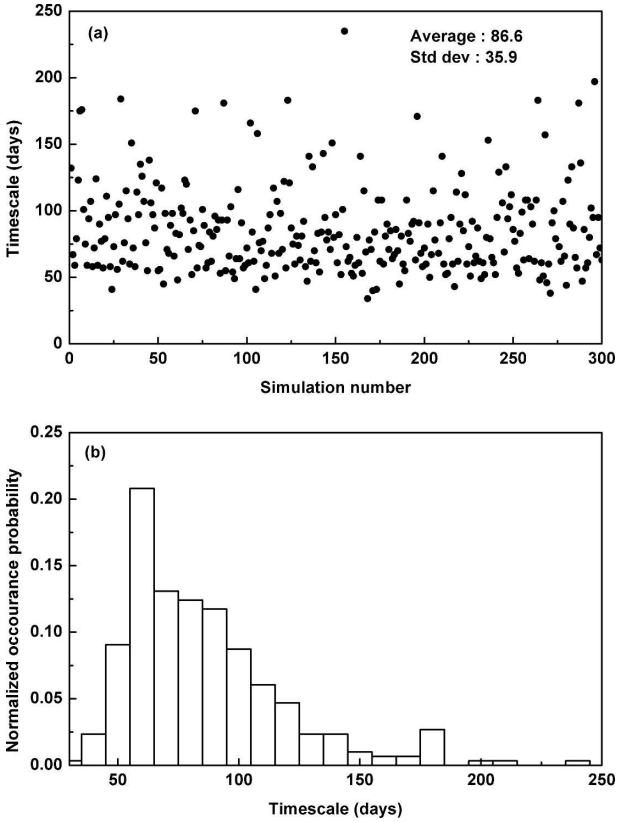

FIG. 1. (a) The response time scale of W_r from (41) for different precipitation input. Each point denotes the time scale calculated from one of the 300 simulations. Simulations differ only in the daily precipitation distribution, while the mean precipitation remains the same as given in Table 1. (b) Normalized occurrence probability of the time scale of W_r in (a).

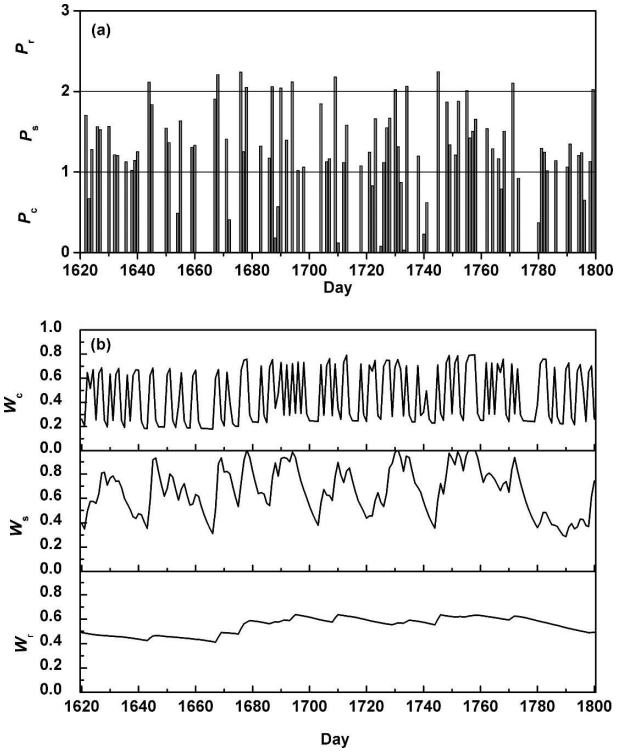

FIG. 2. Normalized time series of (a) precipitation and (b) water content in each layer. Precipitation is normalized by its characteristic value given in Table 1 and the normalized values are separated by increments of 1 from the c layer to r layer for clarity. Water content is normalized by its saturated value (Table 1). For clarity, only the last 180 days (from 1620 to 1800 days) in a 5-yr model integration are shown.

water. Our new time scale $T_2^{**} = 121$ days from (34) is also larger than T_r but is within the 90th percentile partly because the input of precipitation is considered through the mean soil water, as mentioned earlier. This demonstrates that T_2^{**} is a better representation of T_r (i.e., the e-folding response time scale of the root zone soil water) than T_r^*. This conclusion is also supported by additional sensitivity tests in section 6c.

To see more clearly the relationship between the temporal variation of precipitation and those of water content, we randomly take one from the 300 simulations. Time series of daily precipitation partitions are normalized by their critical values (Table 1). For drizzles, all rainfall is intercepted by vegetation. Only for heavy-precipitation events (occurring less than 8% of the time in Fig. 2a) can some rainfall directly reach the root zone through large gaps in the soil. Under this rainfall forcing, the temporal variations of water contents in three layers are quite different (Fig. 2b). The variation of water in the canopy is the fastest among the three layers and closely follows the variation of precipitation in Fig. 2a, while water in the root zone varies slowest.

b. *Spectra analysis of the multiple scales*

To quantify the time scales in the vertical structure of vegetation and soil, power spectra of precipitation, water content, and evapotranspiration are calculated. The spectra are normalized by its total spectra accumulated in all periods, and then divided into four segments: periods <0.2, $0.2 \sim 1$, $1 \sim 3$, and ≥ 3 months. Results from one simulation are given in Fig. 3. Over 70% spectra of the total precipitation and its partitions are concentrated in the high-frequency domain (periods <0.2 months), and only a very small part of spectra are distributed in the low-frequency domain (periods >3 months).

The water contents in different layers show the multiple-time-scale phenomena (Fig. 3b). Most of the spectra (over 60%) of canopy water are concentrated in the short periods. The vegetation canopy holds a small

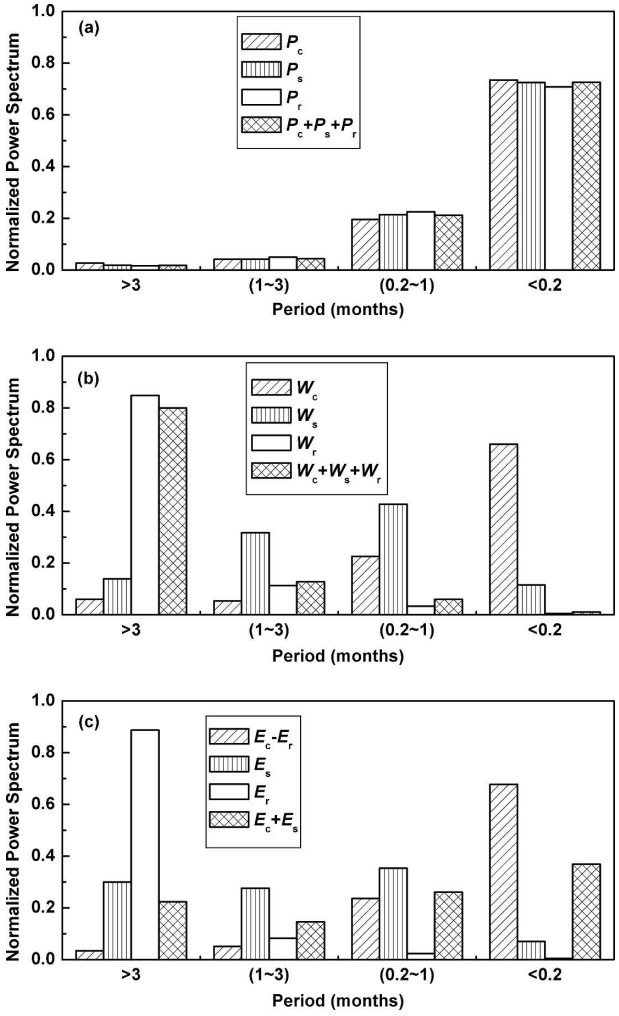

FIG. 3. Normalized power spectra of (a) precipitation and its partitions, (b) water content in each layer, and (c) evapotranspiration, using the same simulation as in Fig. 2.

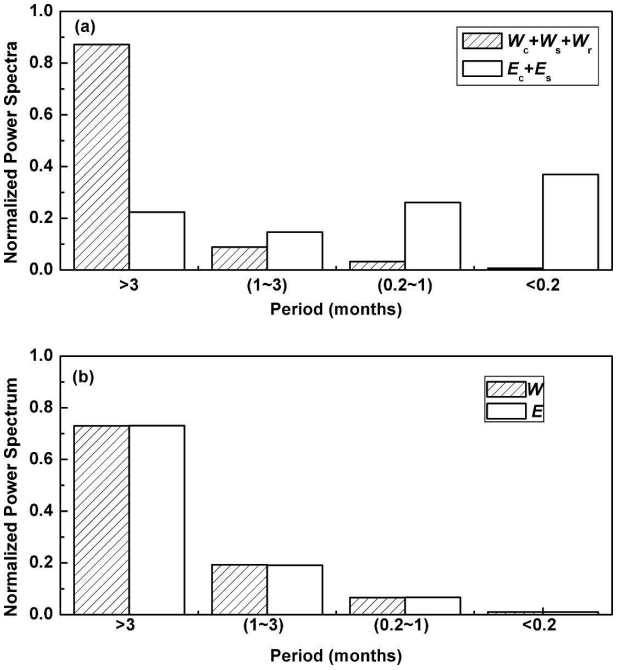

FIG. 4. Normalized power spectra of total water and evapotranspiration produced by (a) the three-layer model [i.e., (10)–(12)] and (b) the one-layer model (15).

amount of water in comparison with the soil, and this water is quickly removed as evaporation. The water stored in the root zone W_r has the longest time scale and most of its spectra are concentrated in the long periods (over 3 months). The water stored in the *s* layer is of intermediate time scale in the three layers. Because the total water is dominated by W_r, its time scale is close to that of W_r. However, the time scale for total water is still smaller than that of W_r, but larger than that of W_s, in agreement with (18).

Figure 3c shows the spectral distributions of evaporation and transpiration. Evaporation from leaves ($E_c - E_r$) includes a large part of short-term components and the intercepted water is quickly evaporated back to the atmosphere. Scott et al. (1997) indicated that time scales associated with evaporation of intercepted water are around one day. Therefore, the spectral distribution of both W_c and ($E_c - E_r$) closely follow that of precipitation in Fig. 3a. Compared with ($E_c - E_r$) and E_s, the variation of E_r has the longest time scale. Even if precipitation is absent, E_r itself could provide some water to canopy. In comparison with E_r and E_s, the spectra of the total evapotranspiration ($E_c + E_s$) are more evenly distributed due to the contribution of the low-frequency E_r and high-frequency canopy evaporation. As the evapotranspiration directly influences the atmospheric processes, therefore, these multiple time scales indeed have different contributions to climate variability on different time scales (Koster and Suarez 1996).

Figure 4 compares the spectra of total water content (i.e., $W = W_c + W_s + W_r$) and evapotranspiration (i.e., $E = E_c + E_s$) from the three-layer model with those in the one-layer model. The spectra distributions of W from both models are nearly the same with most of the spectra concentrated in the low-frequency domain due to the dominance of water content in the root zone of soil. However, the spectra of evapotranspiration from the two models are significantly different. Since the evapotranspiration is a function of water content only, the distribution of E exactly follows that of W in the one-layer model. However, due to the nonlinear interactions among vertical layers in the three-layer model, E and W have very different spectral distributions. Since an important hydrological feedback from vegeta-

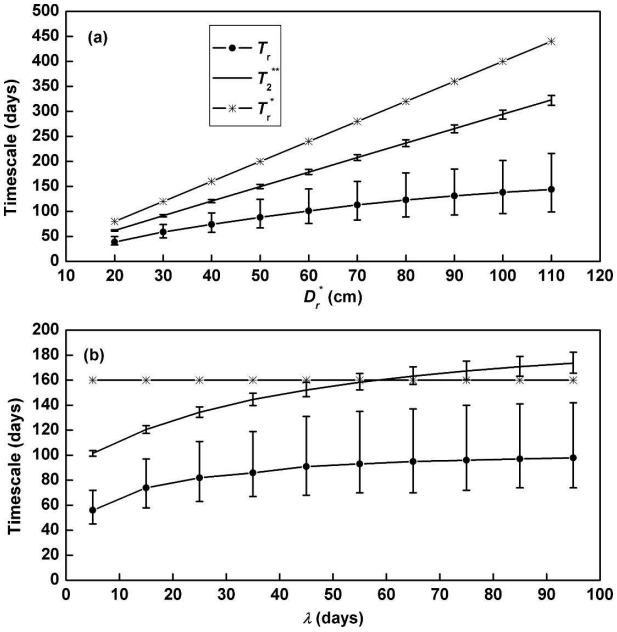

FIG. 5. The variation of time scales of W_r using the same 300 precipitation time series as Fig. 1 along with their interquartile ranges (i.e., the difference between the 75th and 25th percentiles; vertical lines) with respect to (a) depth of r layer D_r^* and (b) interaction time scale (λ) between the s layer and r layer.

tion and soil to the atmosphere is via evapotranspiration, Fig. 4 implies that the one-layer model might incorrectly yield climatic variances in the lower period domain, and a multilayer model is more appropriate for climate modeling.

c. *Sensitivity of time scales of soil moisture to model parameters*

Previous sections have shown that the time scale of soil moisture in the root zone (i.e., T_r) has a relatively long memory in comparison with those of precipitation and surface evaporation, and this time scale is better represented by our new time scale T_2^{**} than by the first-order approximation of T_r^*. Additional simulations are preformed here using the same 300 precipitation series as in section 6a to address the sensitivity of soil moisture time scales to various model parameters.

Figure 5a shows that T_r^* and the median T_r and T_2^{**} all increase with the soil depth of root zone D_r^*, consistent with the results from the analyses of observational data (Vinnikov et al. 1996; Entin et al. 2000; Wu et al. 2002). For the same D_r^*, T_2^{**} is always closer to T_r than T_r^*. Both $(T_r^* - T_r)$ and $(T_2^{**} - T_r)$ increase with D_r^* but the increase of the former is faster. The much smaller interquartile range (i.e., the difference between the 75th and 25th percentiles) of T_2^{**} than that of T_r in Fig. 5a also suggests that T_2^{**} is not sensitive to the random number used to generate the precipitation series in (40).

TABLE 4. Sensitivity of the 25th, 50th (i.e., median), and 75th percentiles of the response time scale (T_r) to various model parameters and formulations. The results are based on the same 300 independent simulations as in Fig. 1. The parameters for the control simulations are OP = 50%, $\overline{P} = 0.33$ cm day^{-1}, $\nu = 0.3$, and $\varepsilon = 0.0$. See the text for additional explanations.

Case	T_r (days)		
	25th	50th	75th
Control	58	74	97
OP: 40%	47	62	81
OP: 60%	61	77	106
$\overline{P} = 0.28$ cm day^{-1}	60	75	99
$\overline{P} = 0.38$ cm day^{-1}	40	54	69
$\nu = 0.1$	58	74	94
$\nu = 0.5$	54	73	94
Delworth and Manabe's (1989) evaporation equation	53	68	88
Add extra runoff $-\varepsilon w_r$ ($\varepsilon = 0.001$)	55	71	90

Figure 5b shows that, while T_r^* is independent of λ (i.e., the interaction time scale of the s layer and r layer), both T_r and T_2^{**} increase with λ. Since $Q_{sr} > 0$ in (11) and (12) most of the time, increasing λ would reduce Q_{sr} (i.e., reduce the amount of higher-frequency soil moisture in the s layer going into the r layer). Therefore, the increasing rate of T_r and T_2^{**} with λ is relatively fast when λ is small. When λ is too large, Q_{sr} is nearly zero, and the increase of T_r and T_2^{**} with λ is relatively slow. Similar to Fig. 5a, the interquartile range of T_2^{**} is smaller than that of T_r.

Table 4 shows that, when the OP is increased from 50% (control) to 60%, the median value and the interquartile range of T_r vary less than those when OP is decreased from 50% to 40%. Overall, the median T_r is not very sensitive to the variation of OP. When the daily mean precipitation $\overline{P}$ is reduced by 0.05 cm day^{-1} (to 0.28 cm day^{-1}), the median T_r varies little. In contrast, when $\overline{P}$ is increased by 0.05 cm day^{-1} (i.e., when soil is wetter) the median T_r is significantly reduced. This asymmetrical behavior agrees with the observed data analysis in Wu et al. (2002) and Wu and Dickinson (2004), which indicated that the dryness signal extends deeper into the soil than the wetness signal and soil moisture time scale can be several times longer for drier conditions than for sufficiently rainy conditions. Table 4 also shows that the median T_r is nearly independent of the infiltration index ν.

We have also analyzed the sensitivity of T_r to some model formulations. Substituting the formula of evaporation (13) by the formulation of Delworth and Manabe

(1989), the median T_r varies by less than 10% (Table 4). As mentioned in section 5, runoff is only considered under supersaturated conditions in the above simulations. A continuous runoff for unsaturated soil can be considered by adding the term $-\varepsilon w_r$ ($\varepsilon = 0.001$) in the right–hand side of (12). Again, Table 4 shows that the median T_r varies little partly because runoff is overall small in the control simulations.

7. Conclusions

Through theoretical analyses and numerical simulations of a three-layer soil–vegetation interaction model, this paper has investigated how land surface hydrology responds to precipitation forcing. The major results are as follows: (a) Different water reservoirs of the vegetation–soil system have different time scales, including very short time scales of canopy water, an intermediate time scale of soil moisture in the surface soil layer, and long time scale of root zone soil moisture. This is consistent with the theoretical conclusion of Dickinson et al. (2003), but cannot be represented properly by the one-layer bucket model. (b) Precipitation forcing is mainly concentrated on short time scales with some small components at low frequencies. However, it can cause the long time-scale disturbances in the soil moisture of root zone, because soil moisture responds more effectively to the low-frequency parts of precipitation spectra, and hence acts as a low-pass filter. (c) The inherent time scale determined by the ratio of the field capacity to the potential evapotranspiration is only a first-order approximation for the response time scale (as defined from the time series analysis). Our new time scale T_2^{**} in (34) considers the vertical interactions between layers as well as the impact of mean soil water (and hence precipitation input), and is indeed closer to the actual response time scale of the root zone soil water (T_r) than the inherent time scale (T_r^*). While T_r can be empirically computed from the soil water time series, it does not provide a clear physical interpretation. In contrast, T_2^{**} is derived directly from our theoretical analysis, and it does provide a physical interpretation of the soil water response time. (d) Comparison of this three-layer model with the one-layer bucket model indicates that the time scale of evapotranspiration is quite different although the time scale of soil moisture itself is very close to each other. This suggests the need to consider the vertical structure in water reservoirs in land surface modeling. (e) The three time scales (i.e., T_r, T_2^{**}, and T_r^*) all increase with soil depth. The first two also increase with the characteristic interaction time scale (λ) between two soil layers (particularly when λ is small), while T_r^* is independent of λ.

While the median T_r is not very sensitive to most model parameters or formulations, it does strongly depend on the mean precipitation rate $\bar{p}$ (particularly when $\bar{p}$ is increased). Therefore it needs to be emphasized that the quantitative results from numerical simulations in section 6 are valid only over midlatitude grassland and they may be different over different regions (e.g., under wetter conditions). However, the theoretical framework and the overall conclusion that T_2^{**} better represents T_r than T_r^* are expected to be valid over different regions.

In this study, we focus on the land surface response to precipitation forcing. When a land model is coupled to an AGCM, the time scales of soil moisture can be different from those in our uncoupled model due to the mutual interactions between land and atmosphere via the atmospheric boundary layer. Dickinson (2000) demonstrated the difference of the time scales for the variability of coupled and uncoupled systems, and concluded that coupling to the atmosphere lengthens the time scale of land. Also missing in our model, just as in many other land surface models (e.g., Zeng et al. 2002), are the horizontal interactions within the soil layers. Similar to the vertical interaction term (14), horizontal interactions would introduce a new time scale. Further study is needed to determine this time scales as well as the impact of horizontal interactions on other time scales discussed in this paper.

Acknowledgments. This work was supported by NASA (NNG04G061G), NSF (ATM0301188), and the China Natural Science Foundation (40233027). The first author also acknowledges support from World Meteorology Organization fellowship. Dr. Xiaodong Zeng is thanked for helpful discussions, and three anonymous reviewers are thanked for their constructive comments that helped improve the manuscript.

REFERENCES

Delworth, T., and S. Manabe, 1988: The influence of potential evaporation on the variabilities of simulated soil wetness and climate. *J. Climate,* **1,** 523–547.

——, and ——, 1989: The influence of soil wetness on near-surface atmospheric variability. *J. Climate,* **2,** 1447–1462.

Dickinson, R. E., 2000: How coupling of the atmosphere to ocean and land helps determine the timescales of interannual variability of climate. *J. Geophys. Res.,* **105,** 20 115–20 119.

——, G. Wang, X. Zeng, and Q.-C. Zeng, 2003: How does the partitioning of evapotranspiration and runoff between different processes affect the variability and predictability of soil moisture and precipitation? *Adv. Atmos. Sci.,* **20,** 475–478.

Entekhabi, D., I. Rodriguez-Iturbe, and R. L. Bras, 1992: Variability in large-scale water balance with land surface–atmosphere interaction. *J. Climate,* **5,** 798–810.

Entin, J., A. Robock, K. Y. Vinnikov, S. E. Hollinger, S. Liu, and

A. Namkai, 2000: Temporal and spatial scales of observed soil moisture variations in the extratropics. *J. Geophys. Res.,* **105,** 11 865–11 877.

Hasselman, K., 1976: Stochastic climate models: Part I. Theory. *Tellus,* **28,** 473–485.

Jiang, S., 1988: *Methodology for Grassland Ecosystem Investigation* (in Chinese). Agriculture Press, 301 pp.

Koster, R., and M. Suarez, 1996: The influence of land surface moisture retention on precipitation statistics. *J. Climate,* **9,** 2551–2567.

——, and ——, 2001: Soil moisture memory in climate models. *J. Hydrometeor.,* **2,** 558–570.

Manabe, S., 1969: Climate and the ocean circulation. I: The atmospheric circulation and the hydrology of the earth's surface. *Mon. Wea. Rev.,* **97,** 739–774.

Milly, P. C. D., 1993: An analytic solution of the stochastic storage problem applicable to soil water. *Water Resour. Res.,* **29,** 3755–3758.

Noilhan, J., and S. Planton, 1989: A simple parameterization of land surface processes for meteorology models. *Mon. Wea. Rev.,* **117,** 536–549.

Scott, R., R. Koster, D. Entekhabi, and M. Suarez, 1995: Effect of a canopy interception reservoir on hydrological persistence in a general circulation model. *J. Climate,* **8,** 1917–1922.

——, D. Entekhabi, R. Koster, and M. Suarez, 1997: Timescales of land surface evapotranspiration response. *J. Climate,* **10,** 559–566.

Serafini, Y. V., and Y. C. Sud, 1987: The time scale of the soil hydrology using a simple water budget model. *J. Climatol.,* **7,** 585–591.

Vinnikov, K. Y., and I. B. Yeserkepova, 1991: Soil moisture: Empirical data and model results. *J. Climate,* **4,** 66–79.

——, A. Robock, N. A. Speranskaya, and C. A. Schlosser, 1996: Scales of temporal and spatial variability of midlatitude soil moisture. *J. Geophys. Res.,* **101,** 7163–7174.

Wu, W., and R. E. Dickinson, 2004: Time scales of layer soil moisture memory in the context of land–atmosphere interaction. *J. Climate,* **17,** 2752–2764.

——, M. Geller, and R. E. Dickinson, 2002: The response of soil moisture to long-term variability of precipitation. *J. Hydrometeor.,* **3,** 604–613.

Zeng, X., M. Shaikh, Y. Dai, and R. E. Dickinson, 2002: Coupling of the common land model to the NCAR community climate model. *J. Climate,* **15,** 1832–1854.

Zeng, X. D., A. Wang, G. Zhao, S. Shen, X. Zeng, and Q.-C. Zeng, 2004: Ecological dynamic model of grassland and its practical verification (in Chinese). *Sci. China Ser. C.,* **34,** 481–486.